Applied Computer Science, vol. 18, no. 4, pp. 82–95
doi: 10.35784/acs-2022-30

Submitted: 2022-10-09 | Revised: 2022-11-27 | Accepted: 2022-12-21

Keywords: pump, CFD, the head of the pump, power, efficiency

Łukasz SEMKŁO [0000-0002-1737-8793]*, *Łukasz GIERZ* [0000-0003-4040-5718]**

NUMERICAL AND EXPERIMENTAL ANALYSIS OF A CENTRIFUGAL PUMP WITH DIFFERENT ROTOR GEOMETRIES

Abstract

The paper presents a comparative analysis of the operation of two variants of centrifugal pump rotors, a description of the main parameters, and the influence of the blade geometry on the performance characteristics obtained. Rotors have been designed using the arc and point method. Based on the developed 3D CAD models, the rotors were printed using the rapid prototyping method on a 3D printer in FFF (Fused Filament Fabrication) technology, in order to experimentally verify the performance, by placing them on the Armfield FM50 test stand. The analysis part of the CFD includes a fluid flow in Ansys Fluent. The process of creating a flow domain and generating a structural mesh was described, along with the definition of boundary conditions, the definition of physical conditions and the turbulence model. The distribution of pressures and velocities in the meridional sections is shown graphically. The chapter with the experimental analysis contains a description of the measuring stand and the methodology used. The results obtained made it possible to generate the characteristics, making it possible to compare the results received. The results allowed to note the influence of geometry on the behavior of the rotors during operation in the system and to indicate that the arc rotor gets a 7% higher head and 2% higher efficiency than the point method rotor, which gives the basis for its commercial use in industry.

1. INTRODUCTION

During development works, CFD computer analysis is more and more often used, which is validated through experimental studies (Cheah et al., 2007). The application of these two methods opens up a wide range of possibilities, as it clearly shows their convergence. CFD analysis allows us to significantly reduce the costs of designing machines and devices. A lot of research work has already been done in which numerical simulation was used to design rotors. The relationships between rotors and stators were analyzed (Zhu et al., 2011), the rotor stabilization itself (Steinbrecher et al., 2003), pump performance under normal and cavitation conditions (Mousmoulis et al., 2021), and critical velocities during pump operation

* Poznan University of Technology, Institute of Thermal Energy, Faculty of Environmental Engineering and Energy, Poznan, Poland
** Poznan University of Technology, Institute of Machine Design, Faculty of Mechanical Engineering, Poznan, Poland, lukasz.gierz@put.poznan.pl

were also analyzed (Song, Zhang & Zhang, 2022). Many other valuable analyzes were also performed (Barmaki & Eghaghi, 2019; Fan & Piao, 2017). In all of such studies, the focus was on numerical analysis. On the other hand, the research work did not forget about experiments related to pumping systems, pumps, and rotors supported by numerical design and analysis (Kaczmarczyk et al., 2019; Ciocan & Kueny, 2006; Li et al., 2020; Bosioc et al., 2019).

The pump is a machine used to pump the medium from the low pressure to the area of higher pressure area. It usually involves the mechanical conversion of electrical energy into hydraulic energy and energy from other sources may also be converted, including e.g., wind force and human strength (Jędral, 2001). The centrifugal pump uses rotating elements to increase torsion (Kijewski, 1993). The increase in angular momentum causes a pressure difference between the inlet and outlet sides, setting the fluid in motion (Ciałkowski et al., 2015). Centrifugal pumps work in a similar way to all turbines; according to Newton's second principle, the fluid flowing through the rotating working organ increases its energy, which is then partially converted into hydrodynamic energy of the fluid flow (Cengel & Cimbala, 2013). The value of its increase depends on the selected rotor structure and rotational speed (Anderson, 1980). There are two families of centrifugal pumps, rotodynamic and circulating (Polish Standard PN-90 / M-44000).

A centrifugal pump was taken into account for the research because it is widely used both in industry and by individual users. Centrifugal pumps are used to transport fluid in central heating systems and water supply systems. They are widely used in the food industry to transport juices, wort, and non-sticky liquids, used for technological processes. The study attempted to design a rotor of such a pump and performed a simulation and experimental analysis. Nowadays, when attention is paid to energy savings, this work is concerned with determining the efficiency of a rotor designed in two variants (point-arc method) and showing which of these variants will be more energy-efficient.

The purpose of this study was to perform a comparative analysis of two rotor variants dedicated to a centrifugal pump using the simulation and experimental method. It was decided to show the influence of two variants of the rotor geometry on the obtained performance characteristics of the centrifugal pump, with an indication of which structure would have a chance to be implemented in the industry.

2. METHODS

2.1. Pomp project

For research purposes, two rotors were designed with different blade curvature. During the preparation of the 3D CAD model, the arc and point methods were chosen. The arc method assumes that the continuity of meridional velocity changes is omitted and the drawing itself takes place by drawing a single arc between the diameters d_1 and d_2. The second chosen method is the method of marking the course of the shoulder blade line according to C. Pfleiderer. This method, used in centrifugal pumps with a single curvature of the blades, consists in assuming a change in the angle β depending on the radius r in the range from r_1 to r_2 and determining the angle ϑ for a given r and β. The values of r and ϑ are the polar coordinates of a given point of the blade and allow to plot the skeleton of the blade.

Table 1 presents the calculation results of two variants of the designed rotors, where characteristic diameters and angles are indicated. Figure 1 shows the meridional section of the rotor determined based on the results obtained from the calculations (see Table 1). Figure 2 shows the geometric interpretation of the blade curvature based on the point method and shows the angle of blade coverage. This angle was determined at the assumption level of $\theta = 69.39°$. Figure 3 shows the angle of blade coverage determined on the basis of the arc method. This angle was determined at the level of $\theta = 24.85°$. The angles shown in both methods have been calculated. The indicated research results were obtained on the basis of relations available in the literature (Troskolański, 1973).

Tab. 1. Calculation results

Parameter	Symbol	Value
Shaft diameter	d_w	15 mm
Hub diameter	d_p	21 mm
Inner diameter	d_1	46 mm
Inlet diameter	d_w	48 mm
Shockless inflow angle	β_1	22°
Plow angle at the outlet	β_2	30°
Outer diameter	d_2	120 mm
Blade width - leading edge	b_1	6 mm
Blade width - trailing edge	b_2	11 mm

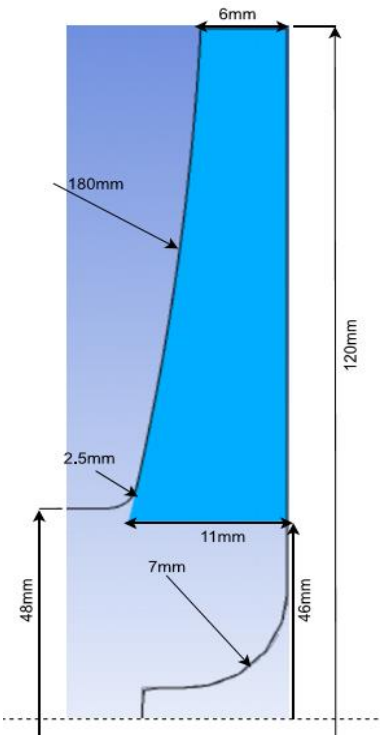

Fig. 1. Rotor meridion cross-section

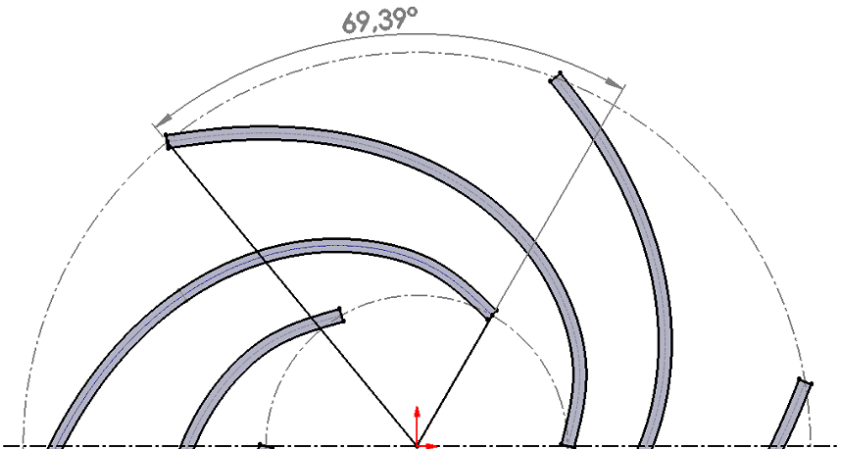

Fig. 2. Blade coverage angle measurement for the point method, θ=69,39°

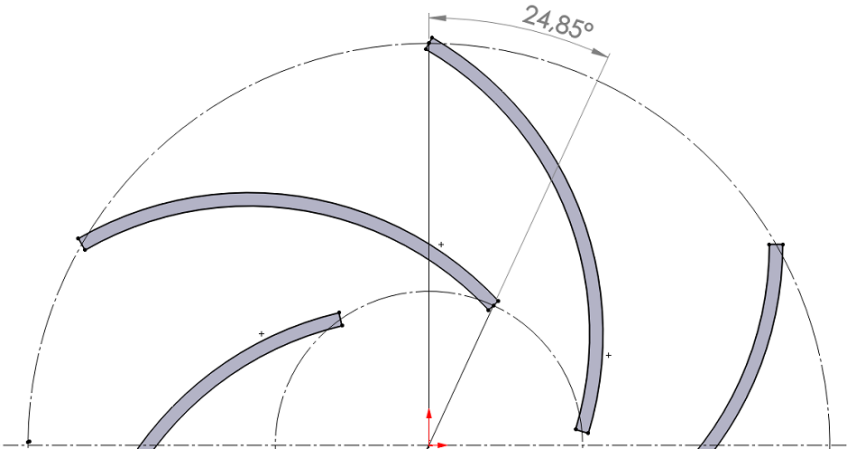

Fig. 3. Blade coverage angle measurement for the arc method; θ=24,85°

2.1. CFD analysis

Numerical analysis was performed in the ANSYS Fluent software (version 19.2). The purpose of the analysis was to compare the behavior of the characteristics of closed rotors with different blade coverage angles, ie, head H, rotor power P, and its efficiency μ. The simulation was performed with the following assumptions: frozen rotor; k-epsilon turbulence model; transported medium – water with a density of 1000 kg/m^3; initial pressure 1 bar; the boundary was taken as p-Total Inlet Mass Flow Outlet. The assumed boundary conditions are shown in Fig. 4. All basic results of the numerical analyzes, i.e., reference diameter, volumetric flow rate, head of the pump H, rotor power P and efficiency μ were collected and presented in Table 2. Based on these data, it can be concluded that the first two parameters are identical, while the next three show differences, where the curved rotor has a higher head of 2.57 m and a lower efficiency of 64.9%, while the point method rotor has a lower head of 2.44 m but a higher efficiency of 66.4%. Figure 5 shows the mesh of one of

the rotors. The tetra net consisted of 230,000 elements. Figure 6 shows the 3D CAD model of both rotors, i.e., made a) with the arc method and b) with the point method. In both rotors, the number of blades is 6 and the main difference between the methods is the radius of curvature of the blades. For the arc method, the radius of curvature is 50 mm, and for the point method it is 60 mm. The value of the radius of curvature of the blades determines their length. So the blades in the arc method are shorter and in the point method the blades are longer. Figure 7 shows the pressure distribution on the discharge side of the pump impeller, while Figure 8 shows the velocity distribution throughout the vane. Based on the numerical analysis using the point method, higher discharge pressure were obtained (Fig. 7). In addition, in the point method, a higher value of the velocity of the fluid in the blade was obtained. It is also possible to observe a uniform velocity distribution in the case of the point method in Figure 8. Analysis of the velocity distribution on the blade for the arc method showed the formation of a local reduction in the velocity value.

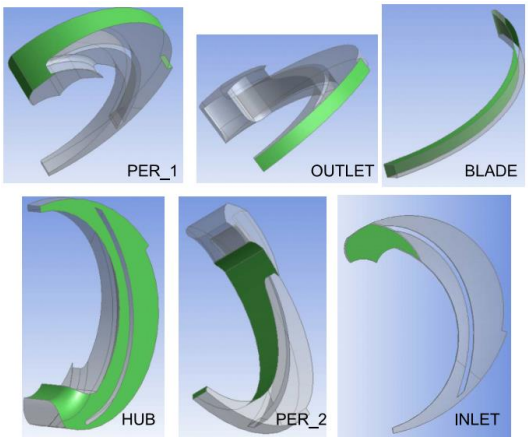

Fig. 4. The assumed boundary conditions

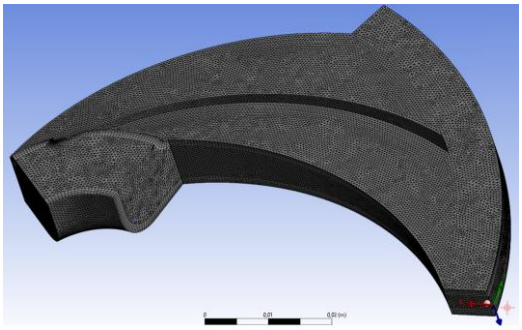

Fig. 5. Calculation grid

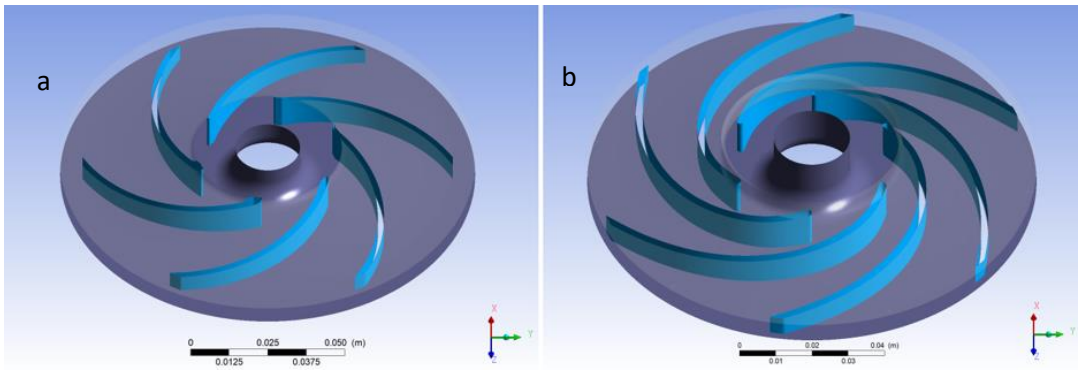

Fig. 6. Isometric view of rotors: a) arc method, b) point method

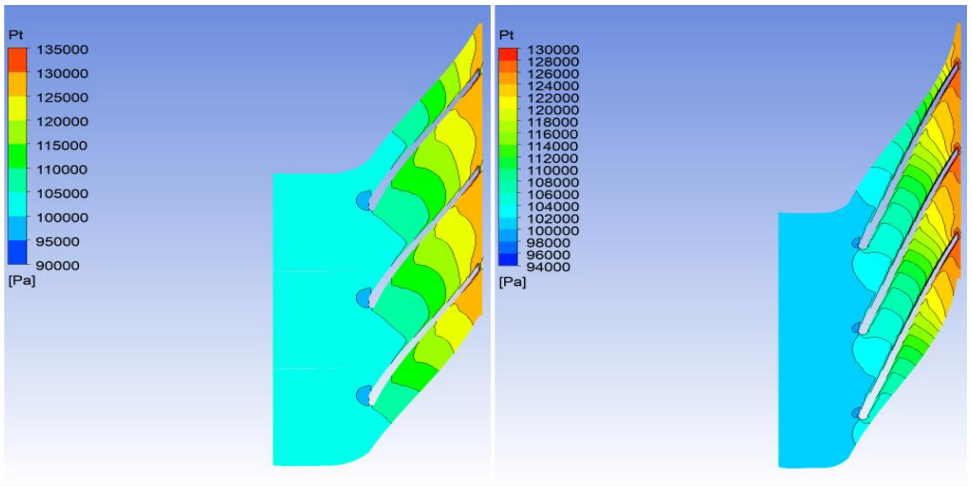

Fig. 7. Discharge pressure P_t: left – arc method; on the right – point method

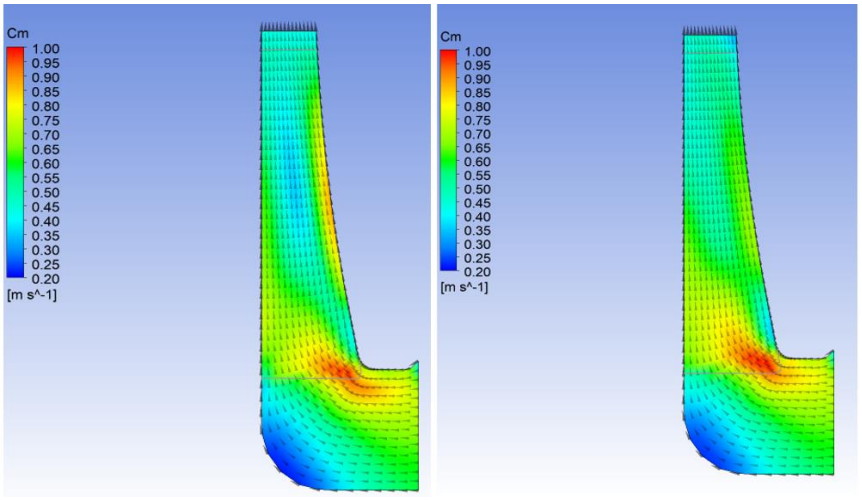

Fig. 8. Velocity vectors on the blade surface: left – arc method; on the right – point method

Tab. 2. The results obtained from the CFD analysis (results for two variants of rotors)

Parameter	Arc method	Point method	Unit
Reference diameter	0.12		m
Volume flow rate	0.0010		m^3/s
Head H	2.57	2.44	m
Power P	25.89	26.28	W
Efficiency μ	64.9	66.4	%

2.2. Experimental analysis

In order to carry out the experiment, the rotors were made using the rapid prototyping method on a 3D printer in FFF (Fused Filament Fabrication) technology. The material used was polylactide PLA, a bioplastic derived from renewable raw materials where additives may be, for example, corn starch or sugar cane.

The tests were carried out on the Armfield FM50 stand. A schematic image of the stand is shown in Figure 9. The system consists of a centrifugal pump driven by an electric motor 4 with a power of 250 W and an acrylic tank 1 with a capacity of 20 liters connected to a small hydraulic system. The water flow through the pump is controlled by a regulating valve in the range of 0 l/min to 96 l/min on the pump discharge side. Manually operated valves at the pump inlet and outlet allow flow control from 0 to 1.6 l/s. The integrated flow sensor allows you to analyze the pump performance and the parameters are controlled using the dedicated FM50 software (Fig. 10), which allows you to record information from the built-in sensors (thermocouple and two pressure sensors), while making the necessary calculations for the needs of the tests. The stand consists of: 1 – reservoir; 2 – control valve on the pump discharge side; 3 – flow meter; 4 – electric motor; 5 – location of the tested rotor; 6 – ball valve on the suction side of the pump; 7 – thermocouple; 8 – base; 9 – tank drain valve; 10 – drainage; 11 – rotor; 12 – drain valve from the rotor body; 13 – pressure measurement on the discharge side; 14 – pressure sensor on the suction side.

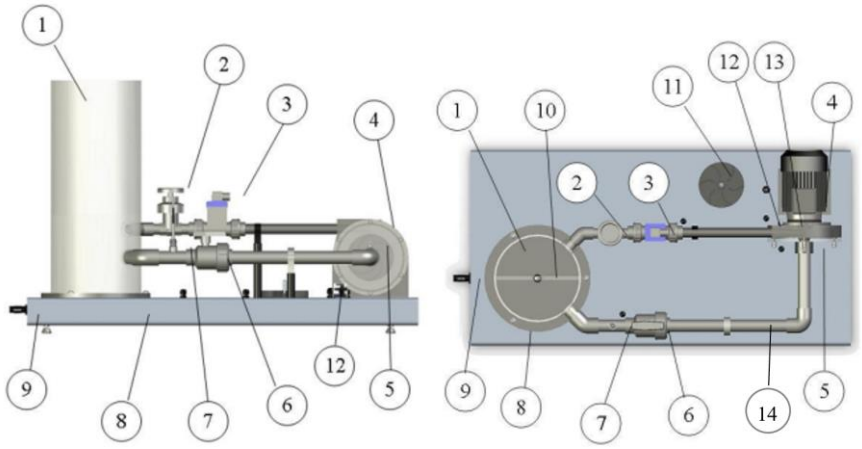

Fig. 9. Diagram of the test stand 1 – reservoir; 2 – control valve on the pump discharge side; 3 – flow meter; 4 – electric motor; 5 – location of the tested rotor; 6 – ball valve on the suction side of the pump; 7 – thermocouple; 8 – base; 9 – tank drain valve; 10 – drainage; 11 – rotor; 12 – drain valve from the rotor body; 13 – pressure measurement on the discharge side; 14 – pressure sensor on the suction side

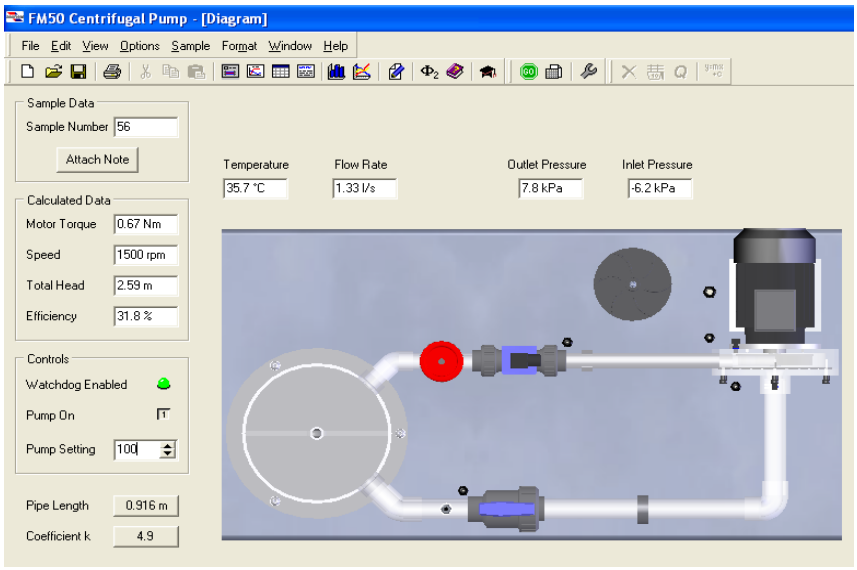

Fig. 10. The Armfield user interface

In order to validate the results of numerical tests (CFD) as part of the planned test program, the discharge part of the pump was throttled through the control valve. This was done by reducing the flow from the maximum value, i.e., 1.0 l/s, in steps of 0.1 l/s, to the set minimum flow value of 0.3 l/s. This procedure was performed with different rotor speed settings: 50%, 60%, 70%, 80%, 90% and 100%. The rotational speeds were similar: 750, 900, 1050, 1200, 1350, 1500 rpm. For each flow tested, the results were recorded (for all the ranges of the pump operation).

On the basis of such a specified test plan, the measurement results presented in Figures 11–18 were obtained. Fig. 11 shows the rotor characteristics for the point method, while Fig. 12 shows the rotor characteristics for the arc method. Thanks to these charts, it can be observed that, in the case of the arc method, it is possible to obtain a higher value of the head by as much as 7% and a better efficiency by 2% compared to the point method. Figures 13–15 show the change of individual characteristics at variable rotational speed for the point method. Figures 16–18 also show the change of individual elements of the pump characteristics at different values of rotational speed for the arc method.

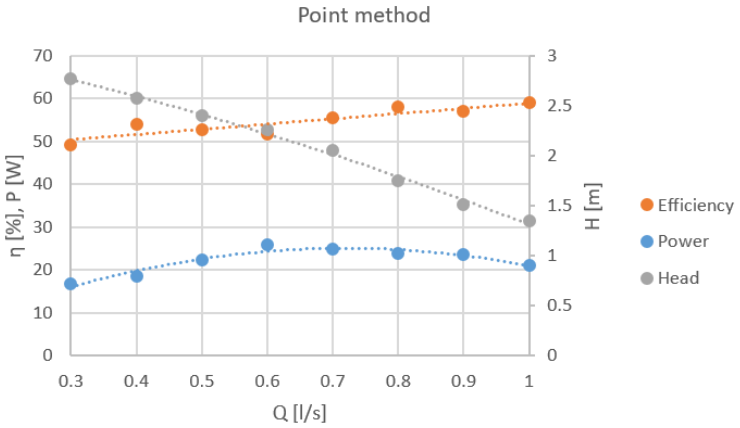

Fig. 11. Pump operation characteristics – point method

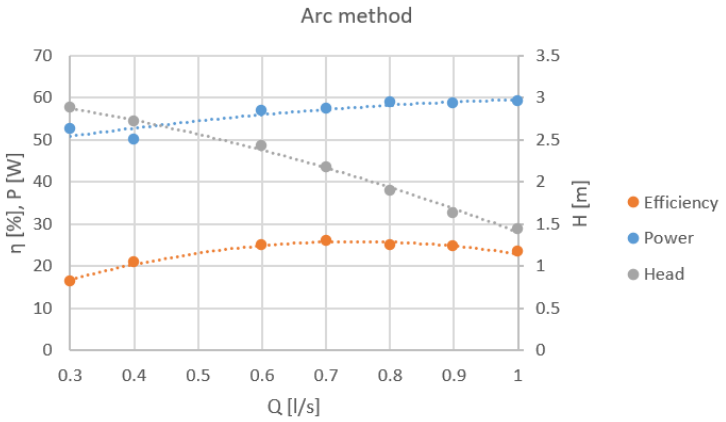

Fig. 12. Pump operation characteristics – arc method

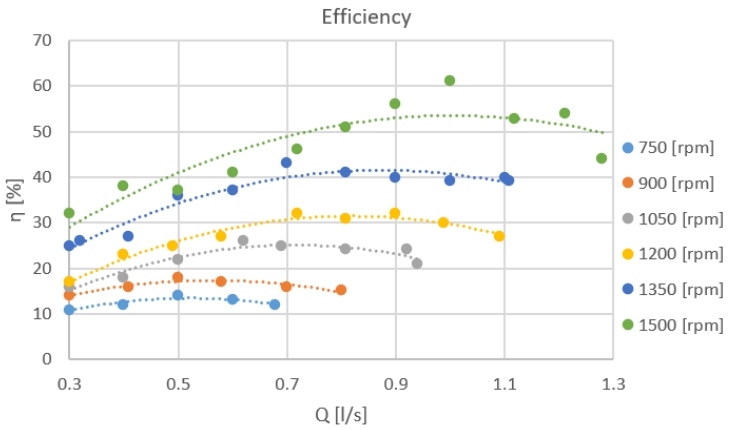

Fig. 13. Efficiency diagram for a rotor designed by the point method at different rotational speeds

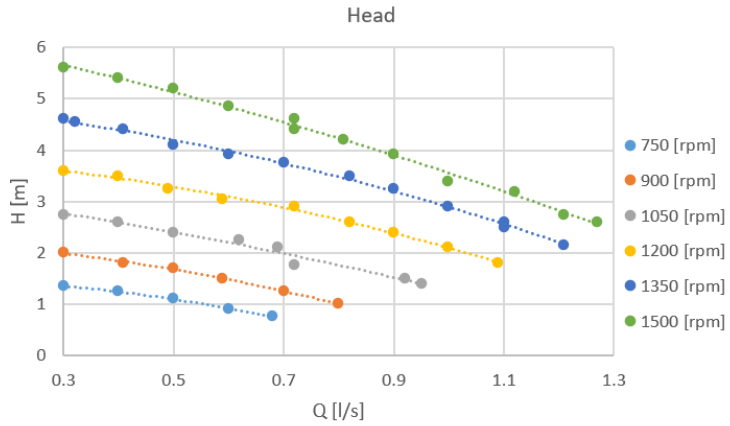

Fig. 14. Diagram of the head of the pump for a rotor designed by the point method at various rotational speeds

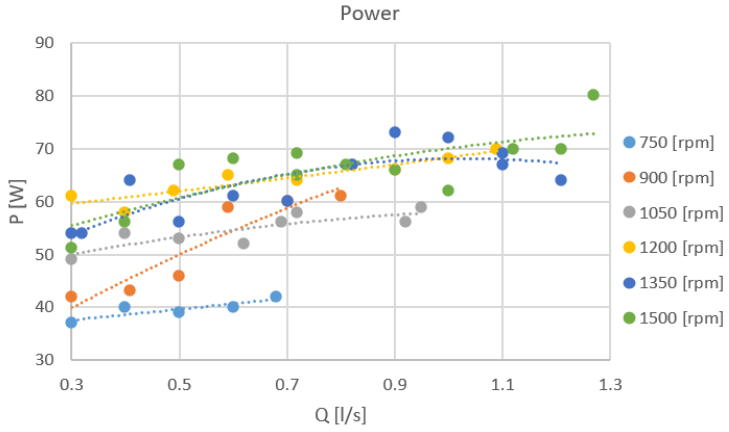

Fig. 15. Power diagram for a rotor designed by the point method at different rotational speeds

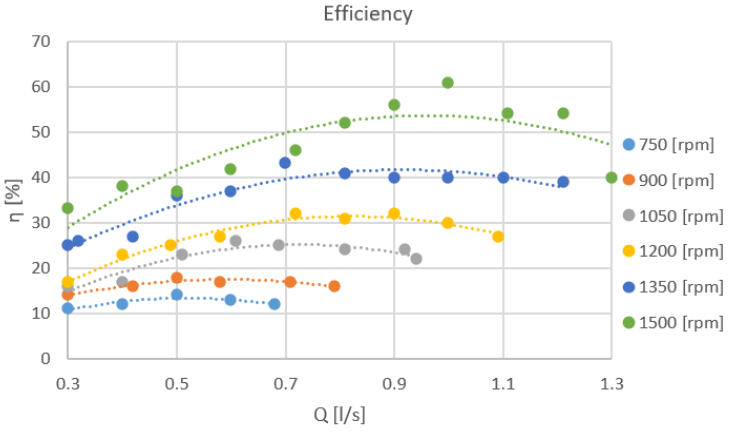

Fig. 16. Efficiency diagram for a rotor designed by the arc method at different rotational speeds

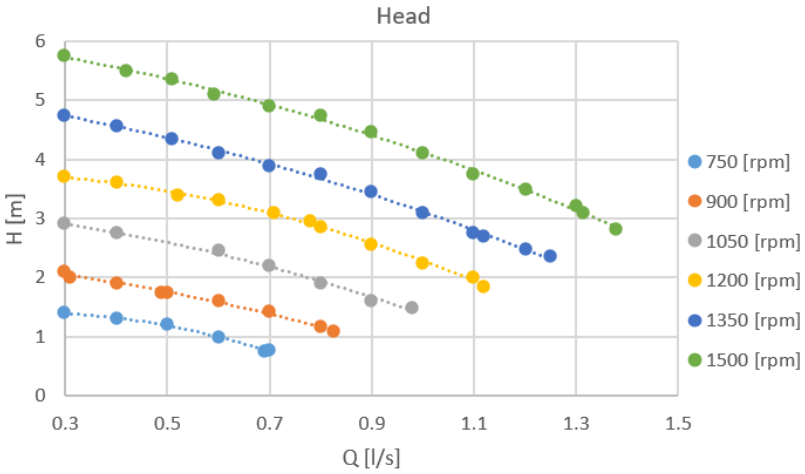

Fig. 17. Diagram of the head of pump for a rotor designed by the arc method at various rotational speeds

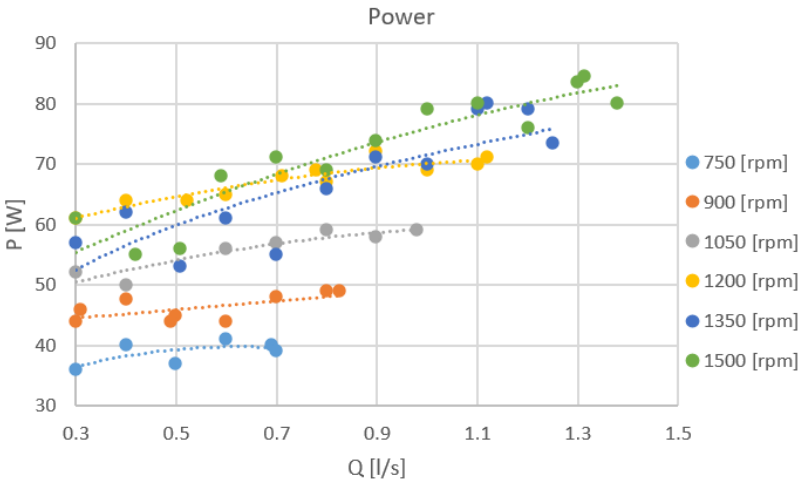

Fig. 18. Power diagram for a rotor designed by the arc method at different rotational speeds

In Figure 13 it can be seen how much influence the change of rotational speed has on the characteristics of the pump. At the lowest speed, the efficiency of the pump, due to the rotor designed by the point method, is from 10 to 14%. Increasing the rotational speed to 1500 rpm increases the efficiency to over 60%. Figure 14 shows the change in the head of pump depending on the rotational speed. At the lowest rotational speed of 750 rpm, the head of the pump H is less than 1.5 m. An increase in the rotational speed causes an increase in the head of pump H up to 5.8 m. Figure 15 shows the change in power generated by the pump. Increasing the engine speed from 750 rpm to 1500 rpm results in a power increase of over 80%.

Almost similar to the point method, the results were obtained for the rotor designed with the arc method. In Figure 16, we can observe an increase in pump efficiency from 10% to over 60%. The same applies for the head of pump. Increasing the rotational speed from 750 rpm to 1500 rpm generates an increase in the head of the pump from less than 1 meter to almost 6 meters. In the case of power in the arc method, the designed rotor increased the power from 35 W to 85 W.

3. DISCUSSION

3.1. Analysis at constant rotational speed

The performed analysis, consisting of the simulation of the flows in the Ansys environment, showed that the head of pump between the rotors (arc and point method) differs by 6%. The higher value of the head of pump of 2.58 m was observed for the rotor with a smaller blade cover angle, i.e. made with the arc method. Despite this, the efficiency of the rotor made by the point method is higher by slightly more than a percentage point. There were no significant differences in pressure distribution and velocity in the meridional sections.

In the experimental analysis the hights of raising at a flow rate of 1 l/s for the closed rotor of the point method and the arc method are 1.35 and 1.44 m. This means that the arc method was characterized by a higher head of pump of approx. 7%, which translates into greater efficiency by 2 percentage points compared to the rotor designed by the second (point) method. The value of the maximum efficiency in the tested flow range for both rotors was identical - although it was obtained for slightly different flows: 0.6l for the point flow and 0.7l for the arc flow. Based on the characteristics for a constant rotational speed of 1050 rpm, a slight influence of the blade shaping method on the performance of the rotor was found. These considerations concern the low specific speed which is 18.8.

Comparing the results of the numerical and experimental analysis at constant rotational speed, it can be seen that the results are convergent. The difference between the results in the case of efficiency in both methods is at the level of 8-9%. The values obtained during the experiment turned out to be lower than the values obtained in the numerical analysis. Interestingly, the situation was reversed in the case of the head of pump. The experimental results are slightly higher than the results obtained in the numerical analysis. The difference is 0.3 meters.

3.2. Analysis at Variable Speed

For the tests performed for variable rotational speed, the efficiency for each rotor was higher the higher the rotational speed. The flow rate corresponding to the maximum efficiency point was the higher the rotational speed. Additionally, higher speeds resulted in an increase in fluctuation and a more irregular course of the curve, making it difficult to estimate the efficiency for points between the flow rates.

The graphs of the head of pump (H) – similar to the efficiency (μ) – show that the increase in rotational speed caused the increase of the tested values. In this case, the changes were more predictable as the increase in rotational speed n contributed to the parallel shift of the curve upward. With the increase of $\dot{Q}$, the difference between successive values of the head of pump H increased – the graph of the course of the hight of increasing increased the slope in relation to the horizontal axis.

The power consumption curve P showed an upward trend with an increase in the flow rate – this applied to each of the tested rotors. Among the characteristics examined, the rotor power P curves had the most irregular course. The rotor designed with the arc method was characterized by the highest power obtained on the pump shaft of the two variants indicated.

3.3. Analysis of experimental studies with CFD

Comparing the experiment (Figures 11 and 12) with numerical calculations, some differences can be noticed. Numerical analysis showed higher values than experimental studies. In the case of the head, the differences in both methods are at the level of 40%. In the case of power, the differences are at the level of 11% for the arc method and 20% for the point method. The smallest difference in results can be observed in the case of efficiency. The difference in results is only 9% comparing the arc method and 11% in the case of the point method.

4. CONCLUSIONS

As part of this study, the performance of a pump was compared, in which two rotors with different parameters (two variants of rotors) were installed. The two types of analyzes performed (simulation CFD and experimental) showed that the designed closed rotors differed slightly from each other for nominal parameters. Both numerical and experimental analysis showed differences in the head of the pump H that did not exceed 7%. In the case of μ efficiency, also the differences were below 2 percentage points for the tested models.

In the experimental analysis, the relative differences between the tested rotors were similar to the results obtained during the simulation tests; however, the absolute values of the head of the pump H were slightly higher by 0.3 meters than indicated by the simulation in the Ansys program. The main reason for these discrepancies is that only the impellers were designed, not the entire pumping system.

In the longer term, the impact of the semi-open impeller on the pump operating parameters should be analyzed, as well as the structure of the entire pump body. Changing the geometry of the pump body could result in increased efficiency.

REFERENCES

Anderson, H. (1980). *Centrifugal Pumps*. Trade and Technical Press

Barmaki, R., & Ehghaghi, M. (2019). Experimental Investigation of a Centrifugal Pump Hydraulic Performance in Hydraulic Transmission of Solids. *Mechanics and Mechanical Engineering*, *23*(1), 259–270. http//doi.org/10.2478/mme-2019-0035

Bosioc, A., Moș, D., Draghici, I., Muntean, S., &Anton, L. E. (2019). Experimental analysis of a pump equipped with an axial rotor with variable speed. *IOP Conference Series: Earth and Environmental Science*, *240*, 032021. https://doi.org/10.1088/1755-1315/240/3/032021

Cengel, Y., & Cimbala, J. (2013). *Fluid Mechanics Fundamentals and Applications*. McGraw Hill.

Cheah, K., Lee, T., Winoto, S., & Zhao, Z. (2007). Numerical Flow Simulation in a Centrifugal Pump at Design and Off-Design Conditions. *International Journal of Rotating Machinery*, *2007*, 083641. http://doi.org/10.1155/2007/83641

Ciałkowski, M., Brodzik, Ł., Wróblewska, A., Frąckowiak, A., Bartoszewicz, J., Joachmiak, M., & Semkło, Ł. (2015). *Mechanika płynów – zbiór zadań z rozwiązaniami*. Wydawnictwo Politechniki Poznańskiej.

Ciocan, G., & Kueny, J.-L. (2006). Experimental Analysis of the Rotor-Stator Interaction in a Pump-Turbine. *23rd IAHR Symposium on Hydraulic Machinery and Systems.* Yokohama, Japan.

Fan, H., & Piao, Y. (2017). Cooling design of an aero-engine fuel centrifugal pump at shut-off. *Advances in Mechanical Engineering*, *9*(6). http://doi.org/10.1177/1687814017709700

Jędral, W. (2001). *Pompy wirowe*. Wydawnictwo Naukowe PWN.

Kaczmarczyk, T., Ihnatowicz, E., Żywica, G., & Kaniecki, M. (2019). Experimental study of the prototype of a Roto-Jet pump for the domestic ORC power plant. *Archives of thermodynamics*, *40*(3), 83–108. http://doi.org/ 10.24425/ather.2019.129995

Kijewski, J. (1993). Maszynoznawstwo. Wydawnictwo Szkolne i Pedagogiczne

Li, W., Ji, L., Shi, W., Yang, Y., Awais, M., Wang, Y., & Xu, X. (2020). Correlation research of rotor–stator interaction and shafting vibration in a mixed-flow pump. *Journal of Low Frequency Noise, Vibration and Active Control*, *39*(1), 72–83. http://doi.org/10.1177/1461348419836530

Mousmoulis, G., Kassanos, I., Aggidis, G., & Anagnostopoulos, I. (2021). Numerical simulation of the performance of a centrifugal pump with a semi-open impeller under normal and cavitating conditions. *Applied Mathematical Modelling*, *89*(2), 1814–1834. https://doi.org/10.1016/j.apm.2020.08.074

Polish Standard PN-90/M-44000. *Przenośniki cieczy.*

Song, H., Zhang, J., & Zhang, F. (2022). Rotor strength and critical speed analysis of a vertical long shaft fire pump connected with different shaft lengths. *Scientific reports*, *12*, 9351. https://doi.org/10.1038/s41598-022-13320-z

Steinbrecher, Ch., Skoda, R., Schilling, R., Müller, N., Breitenbach, A., & Mendler, N. (2003). Numerical Simulation of a Self-Stabilizing Rotor of a Centrifugal Pump. *Proceedings of the ASME/JSME 2003 4th Joint Fluids Summer Engineering Conference* (pp. 71–78). ASME. http://doi.org/10.1115/FEDSM2003-45468

Troskolański, A. T. (1973). *Pompy wirowe*. Wydawnictwo Naukowo-Techniczne.

Zhu, L., Yuan, S., Yuan, J., Zhou, J., Jin, R., & Wang, H. (2011). Numerical simulation for rotor-stator interaction of centrifugal pump with different tongues. *Journal of Agricultural Engineering*, *27*(10), 50–55. http://doi.org/:10.3969/ j.issn.1002-6819.2011.10.009